Synthesis of Degradable poly-HEMA Hydrogels for Tissue Engineering

Zachary Lawrence Wescoe

A thesis

submitted in partial fulfilment of the

requirements for the degree of

Master of Science in Bioengineering

University of Washington

2018

Committee:

Buddy D. Ratner, Chair

James D. Bryers, Chair

Daniel M. Ratner

Program Authorized to Offer Degree:

Bioengineering

University of Washington

Abstract

Synthesis of Degradable poly-HEMA Hydrogels for Tissue Engineering

Zachary Lawrence Wescoe

Chair of the Supervisory Committee:

Professor Buddy D. Ratner

Bioengineering and Chemical Engineering

Co-chair of the Supervisory Committee:

Professor James D. Bryers

Bioengineering

Porous materials have been used as implants to mitigate the foreign body response and improve integration into the host tissue. The foreign body response is characterized by a dense collagen capsule and a chronic inflammatory environment surrounding the implant. This response is mainly mediated by macrophages. Macrophages demonstrate plasticity in phenotype depending on the signals present. The classically activated macrophages are termed M1 and are pro-inflammatory; the alternatively activated macrophages are termed M2 and are pro-healing. Porous materials have been shown to influence macrophage phenotype in a size-dependent

manner with 40μm porous materials showing reduced collagen deposition, increased cellular infiltration, and neovascularization. The positive healing results of non-degradable polyHEMA scaffolds has motivated the construction of degradable scaffolds. A degradable caprolactone-based polyHEMA was previously developed in the Ratner lab, but after one year of implantation intramuscularly, the scaffold had not fully degraded. Ideally, the degradation rate of the material will match the rate of tissue reformation.

This work focuses on the development of another degradable caprolactone-based polyHEMA to explore the tunability of the degradation rate and a new degradable glycolide-based polyHEMA to explore the potential of other degradable esters. The synthesized caprolactone-based polyHEMA performed similarly in degradation studies to the previous caprolactone polyHEMA, indicating minor tunability of degradation rate. There were issues in synthesizing the glycolide-based polyHEMA. These issues arose from the faster degradation rate of the glycolide compared to the caprolactone. Limiting the exposure of the polymer to water was difficult, which lead to premature degradation of the construct. The synthesis reactions need to be further optimized to generate the intended product.

TABLE OF CONTENTS

LIST OF FIGURES

ACKNOWLEDGEMENTS

I would like to thank everyone who aided in the completion of this thesis. Firstly, I would like to thank my advisors, Dr. Buddy Ratner and Dr. James Bryers, for the thoughtful discussions in developing the direction of this project. My thanks are extended to the lab managers, Robyn Francisco, Colleen Irvin, and Sharon Creason, who assisted in general training, ordering of supplies, and upkeep of equipment. Dr. Felix Simonovsky and Dr. Anna Galperin were essential in troubleshooting polymer synthesis issues. Further acknowledgement goes to all of the Ratner and Bryers lab members for helpful discussions and support, especially Dr. Alex Chen, Winston Ciridon, Le Zhen, Dr. Neal Beeman, Ian Dryg, Marvin Mecwan, Lars Crawford, Alissa Bleem, Dr. Vicky Zhang, Razieh Khalifehzadeh, and Thomas Hady. I would also like to thank my many friends I have made along the way here at UW. A special thanks to my housemates, David Peeler, Ian Blumenthal, Kristian Eschenburg, and Patrik Johansson for holding down the fort at Treewalla. Finally, I would like to thank my parents, Dr. Sibyl Wescoe and David Wescoe, for their endless love and support.

Part of this work was conducted at the Molecular Analysis Facility, a National Nanotechnology Coordinated Infrastructure site at the University of Washington with is supported in part by the National Science Foundation (grant ECC-1542101), the University of Washington, the Molecular Engineering & Sciences Institute, the Clean Energy Institute, and the National Institutes of Health. I was graciously funded by the BITE grant from the National Institute of Dental and Craniofacial Research.

DEDICATION

To Momo, my starlight in the darkness.

Introduction

Medicine has used synthetic materials as implants for hundreds of years (Meyer, 2009). Modern tissue engineering can be marked by the development of skin grafts in the 1800s by the surgeon Johann Friedrich Dieffenback (Meyer, 2009). Since then, applications for biomaterials have expanded to include contact lenses, bone screws, cosmetic implants, cell scaffolds, sutures and more. Their use across a broad range of applications has led to the development of an equally broad range of materials. Materials include metals, such as gold and titanium, ceramics, such as hydroxyapatite and tricalcium phosphate, synthetic polymers, such as acrylates and polyurethanes, and natural polymers, such as collagen and agarose (Saini, 2015). These materials are chosen based on their application: metals and ceramics are used in bone settings, while polymeric hydrogels are used in soft tissues (O'Brien, 2011). Interestingly, the same material into a different microstructure can lead to a different healing outcome. Biomaterials have been manufactured into a variety of shapes and architecture, including solid, porous, electrospun fibers, woven meshes, and microspheres.

The first tissue engineered material was approved by the FDA in 1998 (Zaulyanov and Kirsner, 2007). The Apligraf is approved for use to treat chronic venous leg and diabetic foot ulcers and is composed of a collagen matrix cultured with neonatal fibroblasts and neonatal epidermal keratinocytes. This forms a bilayer system to mimic the native epidermis and dermis. This graft is placed on the ulcer to promote healing. After 4 weeks, the graft has been fully replaced by patient tissue. Although this graft enhances the healing of diabetic ulcers, it does have some drawbacks. The use of neonatal fibroblasts necessitates cellular expansion *ex vivo*, which is costly and the use of allogenic cells carries the risk of immune rejection, although the Apligraf has shown limited immune response.

To alleviate issues associated with cell-seeded scaffolds, polymer systems were developed. The Integra matrix is composed of collagen and glucosaminoglycan with a surface layer of silicone to prevent water loss (Berthiaume et al., 2011). This matrix allows for patient cells to infiltrate into the matrix from the edges of the skin wound. As fibroblasts move into this space, they break down the matrix and regenerate the dermis. After the dermis has regenerated, the silicone layer is removed and the epidermis completes formation.

Biomaterials have shown extensive regeneration potential, however, materials implanted in the body induce the foreign body response. This response is characterized by a chronic inflammatory state at the surface of the implant and a dense collagen capsule walling the implant off from the body (Anderson et al., 2001). Immediately after implantation, serum proteins adsorb onto the surface of the implant and neutrophils are recruited to the area due to damage associated molecular patterns (Lee and Kim, 2014). Neutrophils secrete pro-inflammatory cytokines which attract monocytes to the implant and induce differentiation into macrophages. In response to the adsorbed proteins, macrophages attempt to phagocytose the implant by fusing into foreign body giant cells and continuing to secrete pro-inflammatory cytokines. These cells secrete factors that recruit and activate fibroblasts to lay down a collagen matrix. As this process continues, a dense collagen capsule forms around the implant (Lee and Kim, 2014).

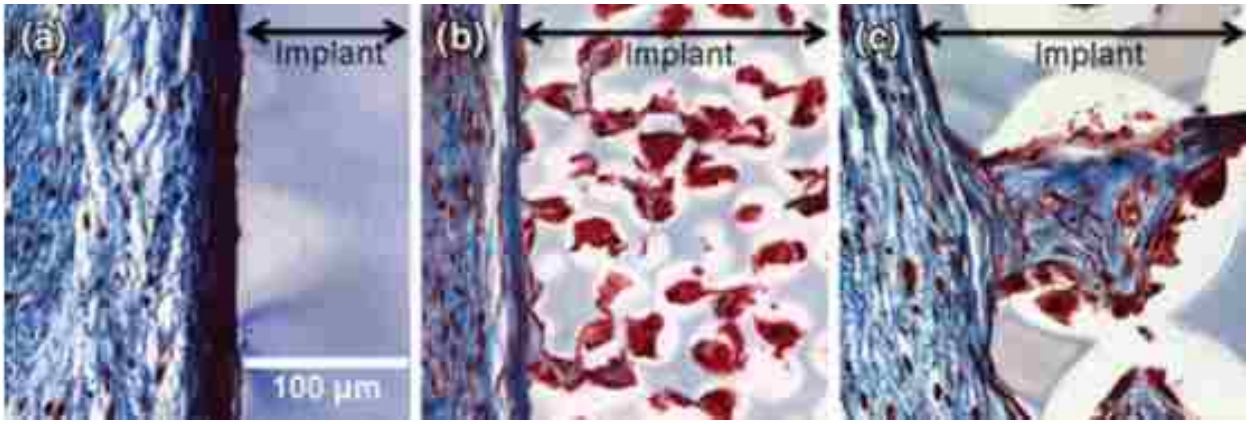

The foreign body response is mainly mediated by macrophages. Macrophages exhibit extensive plasticity in their phenotype and fall into two main groups: pro-inflammatory M1 and pro-healing M2 phenotypes (Wynn and Vannella, 2016). TNF-α and interferon-γ induce the M1 phenotype while interleukin-4 and interleukin-13 stimulate the M2 phenotype. Can biomaterials aid in the transition from inflammation to proliferation to avoid the foreign body response? Can biomaterials affect macrophage phenotype?

Poly-2-hydroxyethyl methacrylate (polyHEMA) is a prominent hydrogel for soft-tissue biomaterial applications. It has mechanical properties that match many biological tissues (Young et al., 1998). It shows good elasticity, is FDA approved, and is easy to fabricate through radical polymerization.

Background

To explore the effect of biomaterial pore size on tissue integration, Sussman et al. created polyHEMA scaffolds with different microstructures – non-porous, controlled 40μm pore, and controlled 160μm pore – and implanted them subcutaneous in mice for 3 weeks. Upon explantation, Masson's trichrome stain was used to assess cellular ingrowth and collagen matrix deposition (Fig. 1). The non-porous polyHEMA implant was surrounded by a dense collage capsule. The 160μm polyHEMA implant allowed for cellular ingrowth, but there was significant deposition of collagen within the porous matrix. The 40μm polyHEMA implant, however, supported cellular ingrowth with a limited collagen layer at the surface of the implant (Sussman et al., 2014).

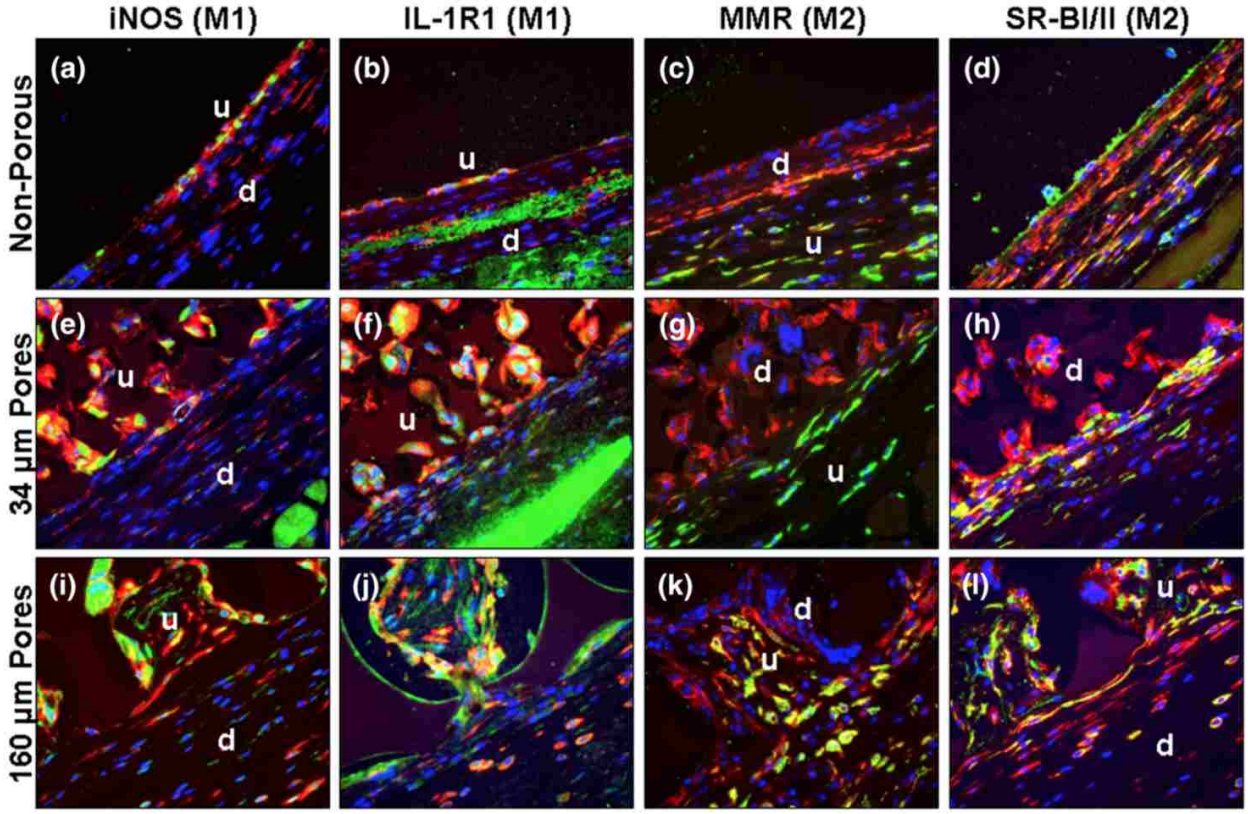

To assess the macrophage population around and within the implant, Sussman et al. used immunohistochemistry to identify two M1 markers, inducible nitrous oxide synthase and IL-1 receptor, and two M2 markers, macrophage associated mannose receptor and scavenger receptor BI/II (Fig. 2). As expected, the non-porous implant showed an increased M1 phenotype and a decreased M2 phenotype at the surface of the implant, indicative of the foreign body response. The porous implants showed an increase of M2 phenotype markers at the surface of the implant while there was an increased M1 phenotype markers within the pores of the implant.

Further, porous materials implanted into the heart myocardium supported neovascularization in a pore-size dependent fashion (Madden et al., 2010; Fig. 3). The thinnest capsule was found in the 20µm and 30µm porous polyHEMA implants, while the 60µm and

non-porous implants induced capsule formation. The 30μm porous polyHEMA also supported the most neovascularization. This demonstrates that there are physical cues from the porous architecture that induce healing, or at least, limit the damage.

Additionally, a 40μm porous rod was implanted transcutaneously on the back of a mouse to assess the ability of porous polyHEMA to regenerate the native tissue architecture (Fukano et al., 2010). Keratinocytes were found within the porous matrix adjacent to the epidermis while laminin 332 was found within the pores at the interface between the epidermis and dermis. Thus, controlled pore size scaffolds can reduce the foreign body response, allow cellular ingrowth, and support cellular differentiation to reform the native tissue architecture.

Ideally, new tissue can regrow in the implant area and take over from the scaffold. With the success of the non-degradable porous polyHEMA scaffolds, there is motivation to develop a degradable version. Polyesters have been used as degradable scaffolds but have some limitations for tissue engineering. They do not have elastomeric properties and do not match the mechanical properties of tissues. When they break down, they produce acidic products that are not

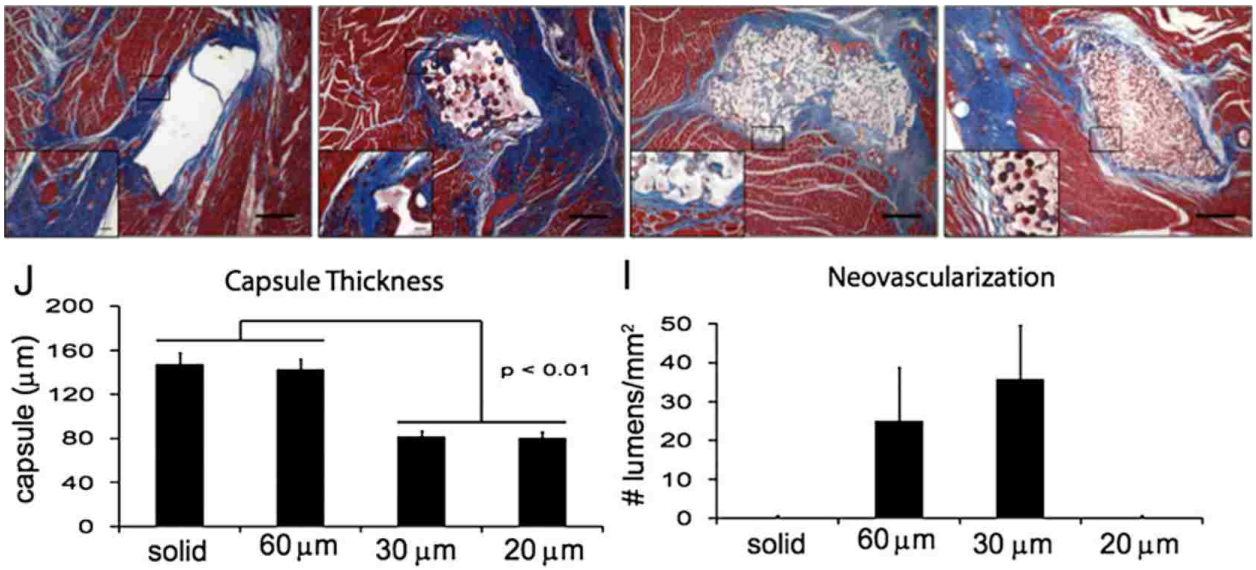

conducive to cell growth. Additionally, the acidic breakdown products catalyze further degradation. Finally, they are hydrophobic and do not lend themselves to hydrogel formation (Atzet et al., 2008).

Atzet et al. developed the design of a degradable crosslinker and a degradable macroinitiator for the synthesis of a degradable polyHEMA (Fig. 4). The presence of caprolactone in the core of the crosslinker and macroinitiator allows for hydrolysis. The macroinitiator is used to polymerize HEMA using controlled radical polymerization to ensure that the final degradation products are small enough such that they are soluble and able to be cleared from the body.

The porous caprolactone-based degradable poly-HEMA was implanted intramuscularly in mice. After 18 weeks, the scaffold supported cell ingrowth, but there was minimal degradation (Atzet thesis, 2008; Fig. 5). This spurred the development of a quicker degrading version based on poly-lactic acid. After 1 week of implantation the PLA-based degradable poly-HEMA had fully degraded with minimal tissue reformed in the area. This can be attributed to the degradation products needing to be removed prior to healing (Atzet thesis, 2008; Fig. 6).

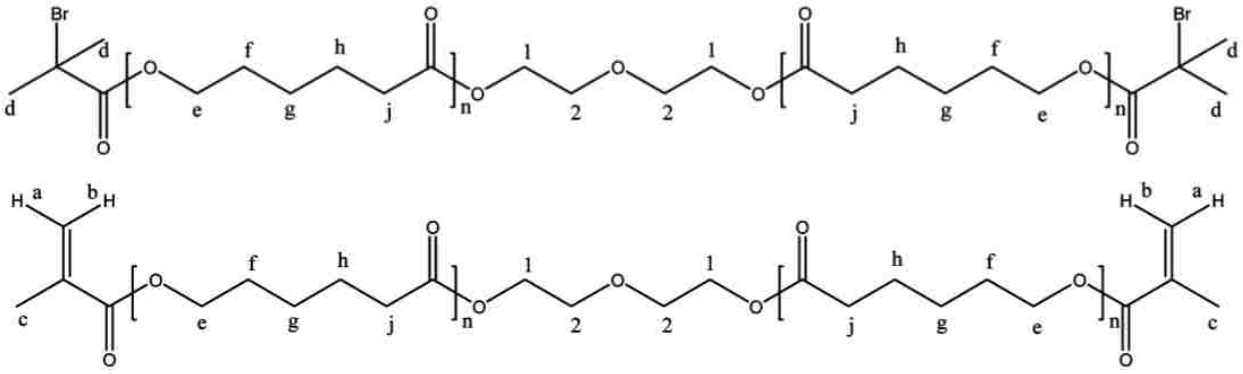

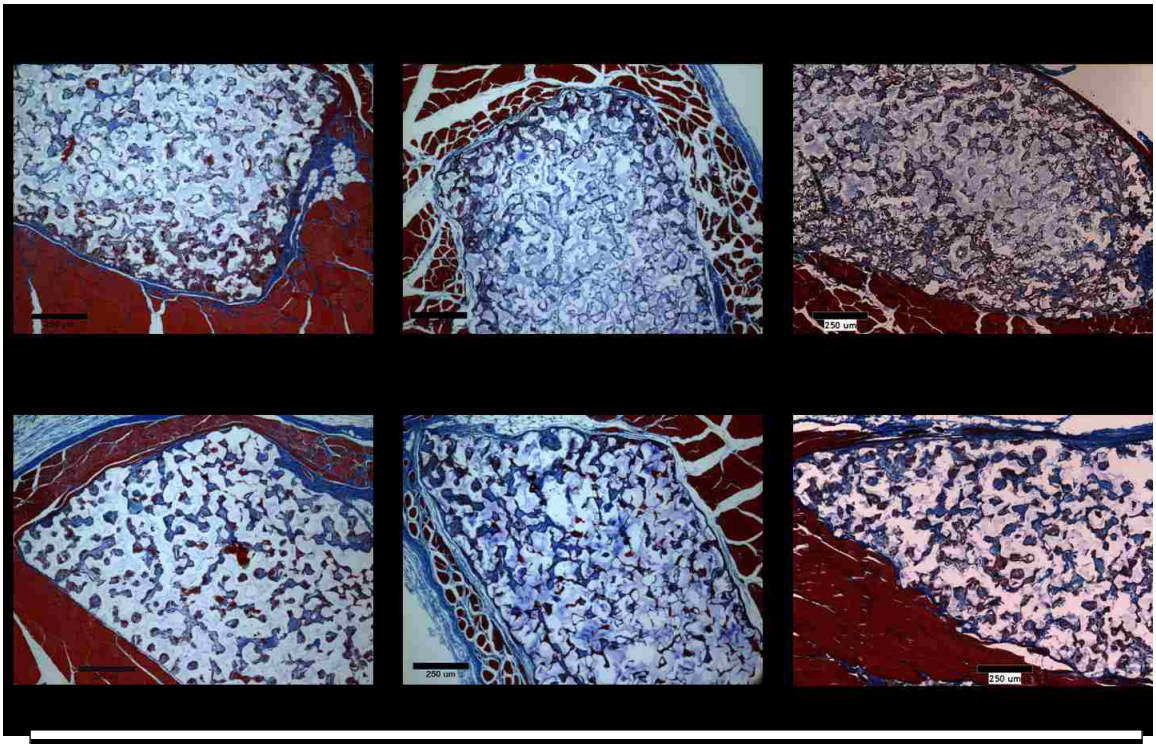
250 um
250 um
250 um

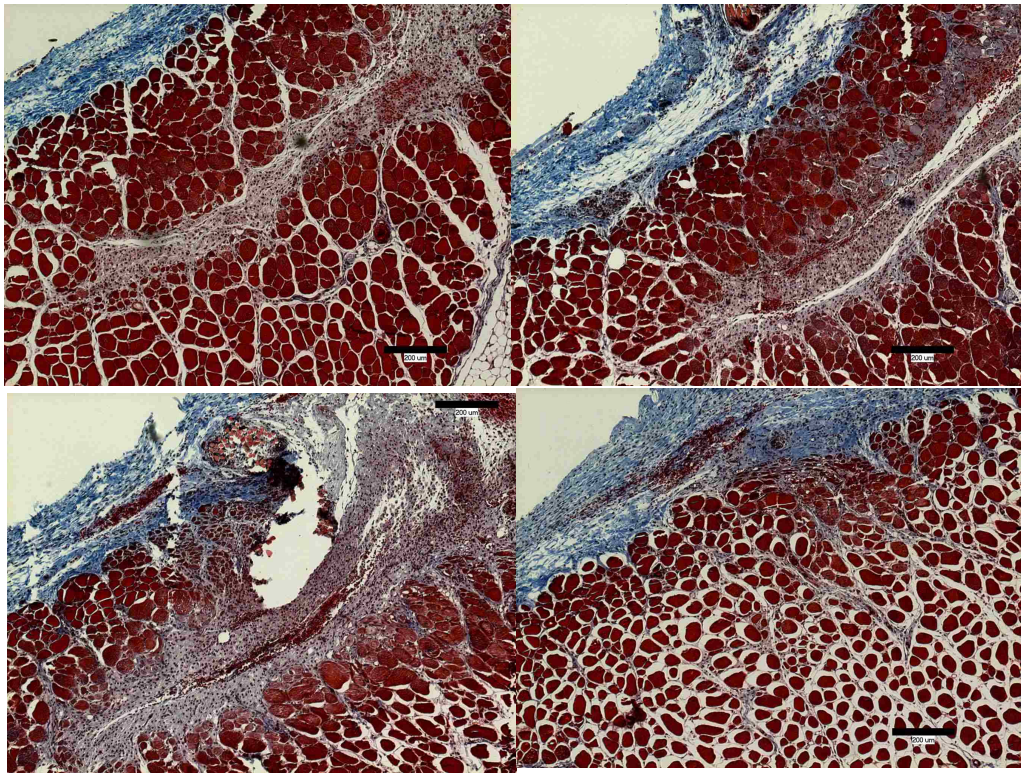
200 um
200 um
200 um
200 um

Based on these results, a scaffold that degrades slower than the lactic acid-based polymer and faster than the caprolactone based polymer is desired. To explore this, I developed another caprolactone-based macroinitiator and crosslinker as well as a poly-glycolic acid based macroinitiator and crosslinker using Atzet's design.

The degradable caprolactone-based polymers increased the ethylene glycol units from two to six, to increase the hydrophilicity of the polymer, and increased the caprolactone units from two to five on each side, to increase the number of cleavable sites. Similarly, the glycolide-based polymers contained six ethylene glycol units and five glycolic acid units on each side.

Results

Caprolactone-based degradable hydrogels

The ATRP reaction to synthesize the caprolactone-based degradable polyHEMA failed due to the presence of oxygen within the glove box. As a result, I switched to the ARGET ATRP method which includes a reducing agent to regenerate the oxidized copper complex. After switching to this polymerization method, I was able to generate porous, degradable polyHEMA scaffolds (Fig. 7).

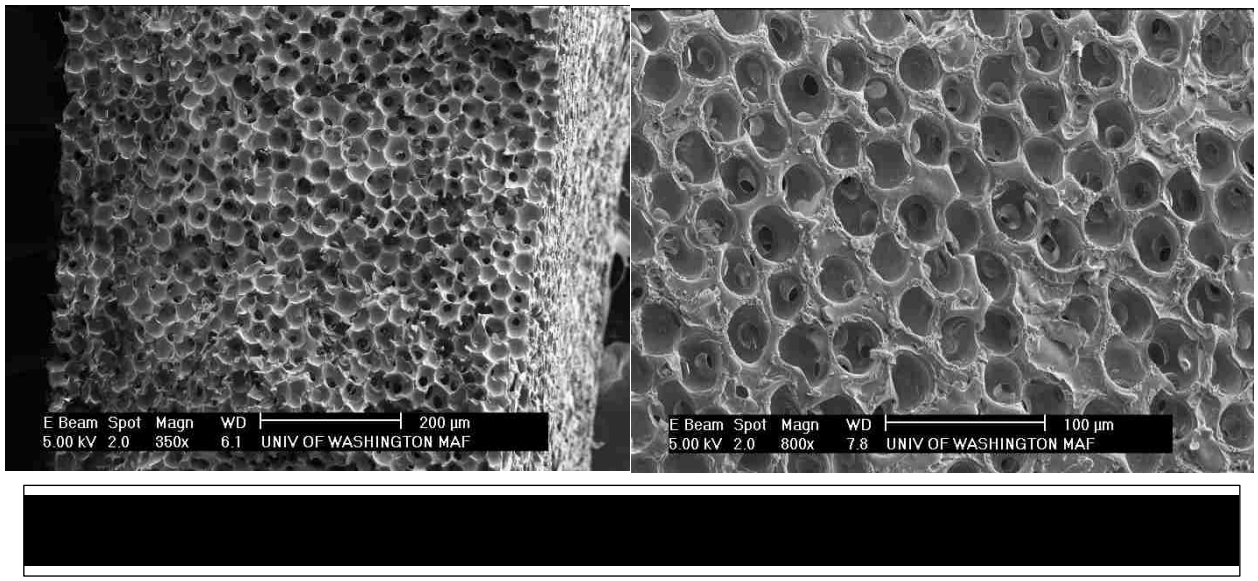

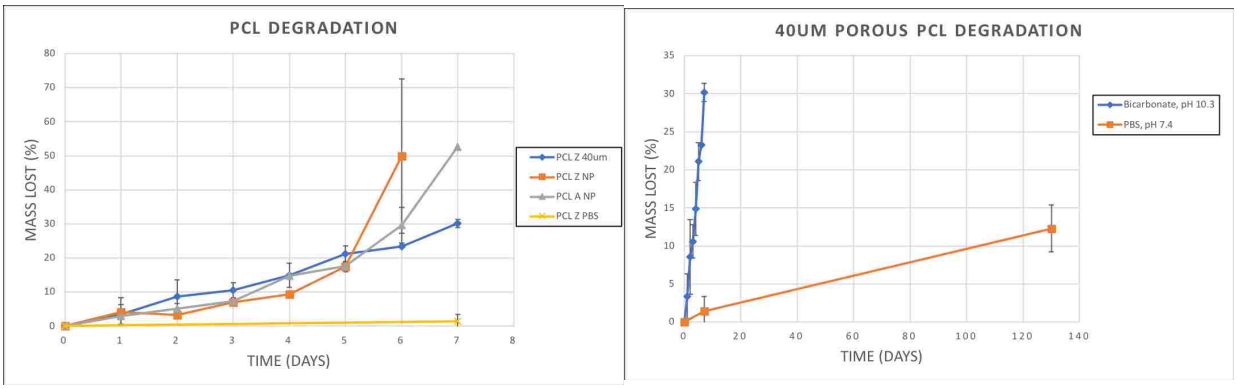

[redacted]

Despite the differences in polymer design between Atzet's poly-caprolactone and my poly-caprolactone degradable polyHEMAs, there was not a significant difference in degradation rates (Fig. 8) in the accelerated degradation study. Both scaffolds lost the same amount of mass by the 6-day time point and scaffolds had lost their structural integrity. There was minimal degradation in PBS, although after four months, the scaffold had lost about 12% of its mass.

Glycolide-based degradable hydrogels

When I attempted the ARGET ATRP using the PGA-based crosslinker and ATRP initiator, there was no polymerization. To assess why the scaffold didn't polymerize, I ran NMR on the ATRP initiator (Fig. 9) to ensure that the α-bromoisobutyryl bromide was added to the polymer. The relative intensity of the peaks corresponding to the interior PEG protons (a, 16 hydrogens) and terminal methyl protons (e, 12 hydrogens) is expected to be 4/3, but instead is 2.6966/1.6453 = 1.63. This indicates that not all ATRP initiator molecules are bifunctional, but many of them are. The polymerization issue isn't due to poor functionality of the ATRP initiator. However, another comparison we can do is between the peaks for the interior PEG protons (a, 16 hydrogens) to the glycolide protons (d, 16 hydrogens). We expect a 1:1 ratio of the peaks, but we instead see a 2.6:1 ratio with over representation of the interior PEG protons.

This is a minor concern, though, because there is enough signal from the d protons that the ATRP initiator is degradable.

Next, I evaluated the crosslinker (Fig. 10) in a similar manner. The relative intensity of the peaks corresponding to the interior PEG protons (a, 16 hydrogens) and terminal methyl protons (f, 6 hydrogens) is expected to be 16/6 = 2.67, but instead is 27.5081/3.0669 = 8.97. This indicates that a majority of the crosslinker molecules only have one methacryloyl group conjugated, which doesn't make the molecule a crosslinker. Additionally, we can compare the glycolide protons (d, 12 hydrogens) to the terminal glycolide protons (e, 4 hydrogens). We would expect a 3:1 ratio, but we instead see more signal from the e protons. This indicates that some of the crosslinker molecules degraded prematurely and may only have one glycolic acid group attached to the PEG.

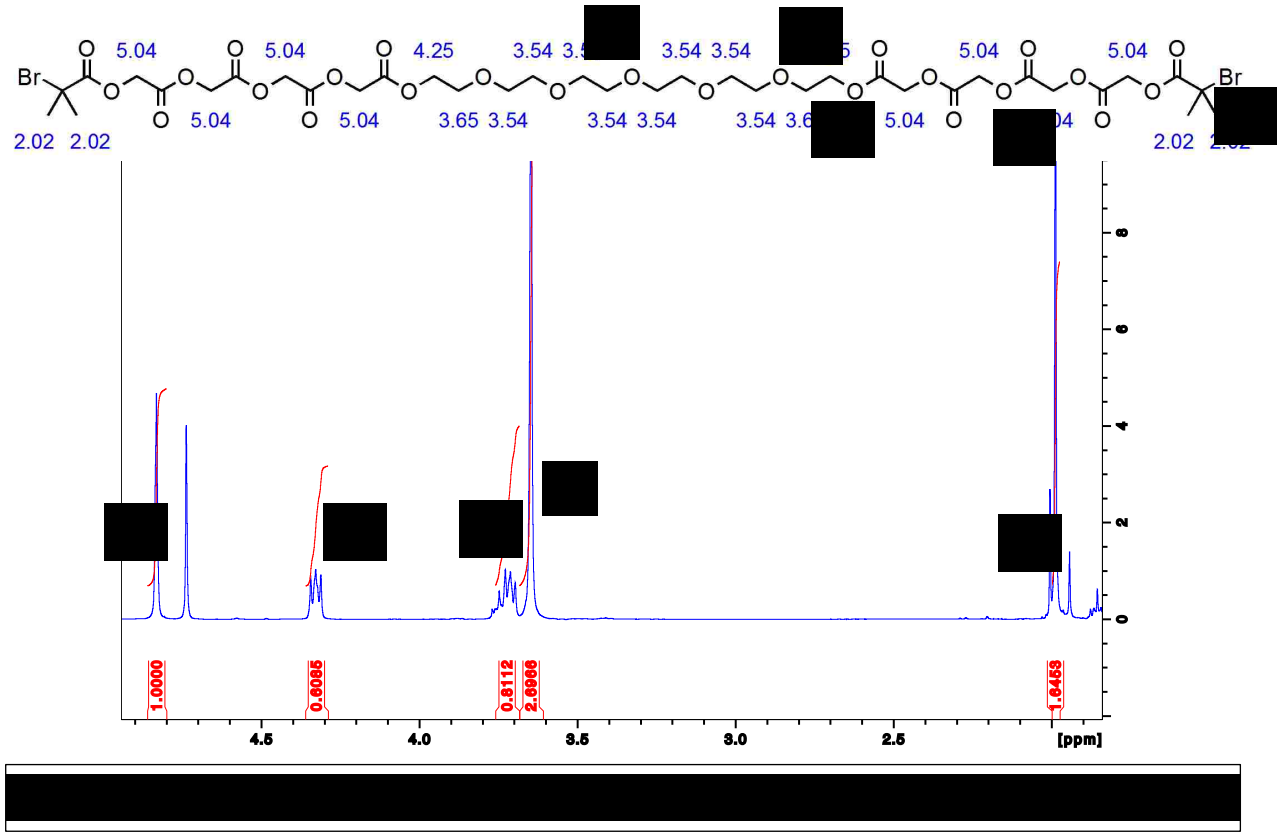

Based on the poor representation of the glycolide protons in the crosslinker, I also analyzed the PEG-glycolic acid diol used to synthesize the crosslinker (Fig. 11). The relative intensity of the peaks corresponding to the glycolide protons (e, 4 hydrogens) and the interior PEG protons (a, 16 hydrogens) is expected to be 4:1, but instead is 6.9633/1.4065 = 4.95. This indicates that there was poor conjugation of the glycolide to the PEG in the initial synthesis step.

Conclusions

In the accelerated degradation study, the two caprolactone-based degradable polyHEMAs performed similarly. This could be due to their degradation kinetics being the same, however, it is possible that the accelerated conditions masked the minor differences in overall degradation rate.

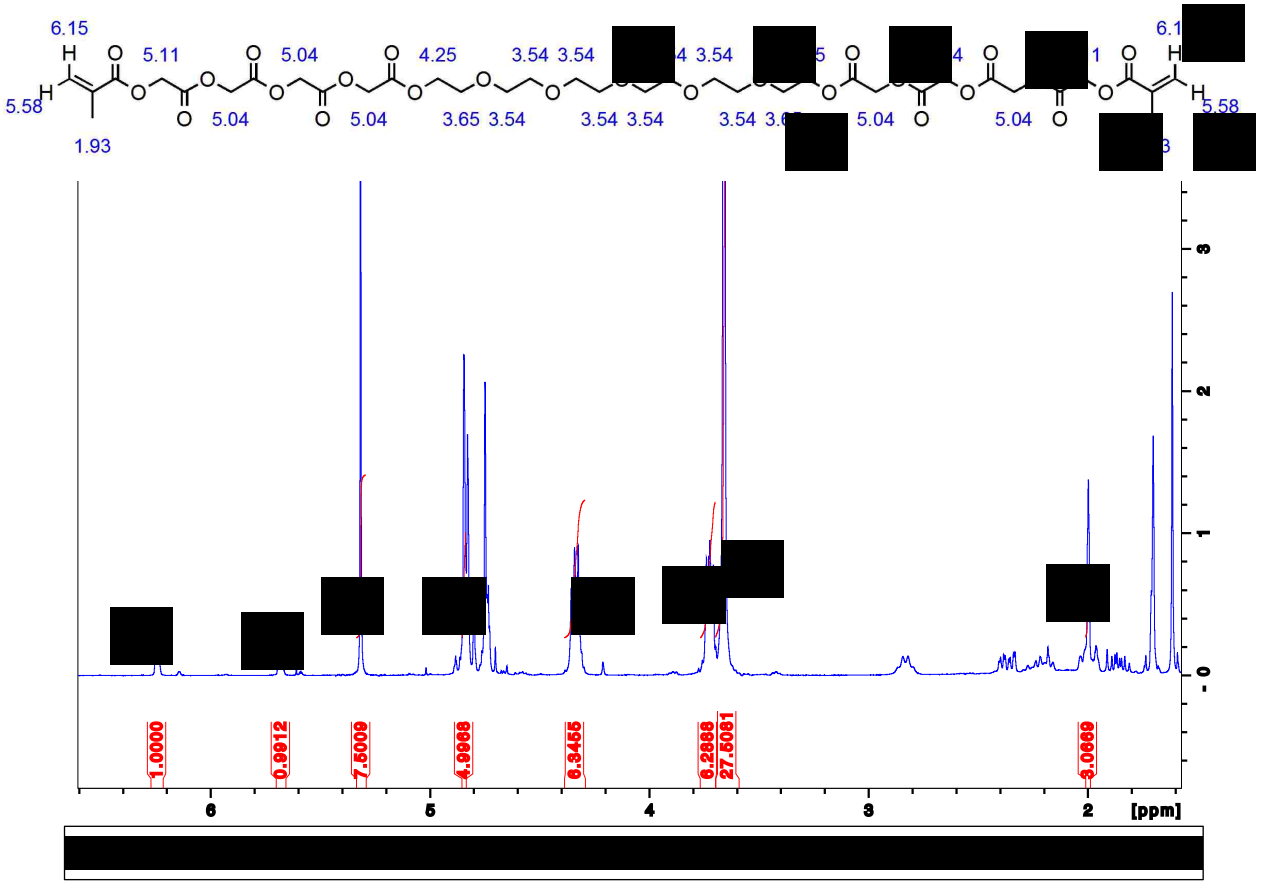

There were polymerization issues with the glycolide-based degradable polyHEMA. In the ARGET ATRP reaction, the culprit was the poor functionality of the synthesized crosslinker not the ATRP initiator. It was unclear, initially, whether the reaction to add the methacryloyl chloride to the diol was flawed or if the polymer was degrading during purification after the reaction. The ATRP initiator and crosslinker are purified using the same procedure, so if it were the purification step, it should have affected both, but only the crosslinker was affected. Thus, it had to be something specific to the crosslinker reaction. Methacryloyl chloride is highly moisture sensitive and could have been deactivated by moisture before it had a chance to add to the diol.

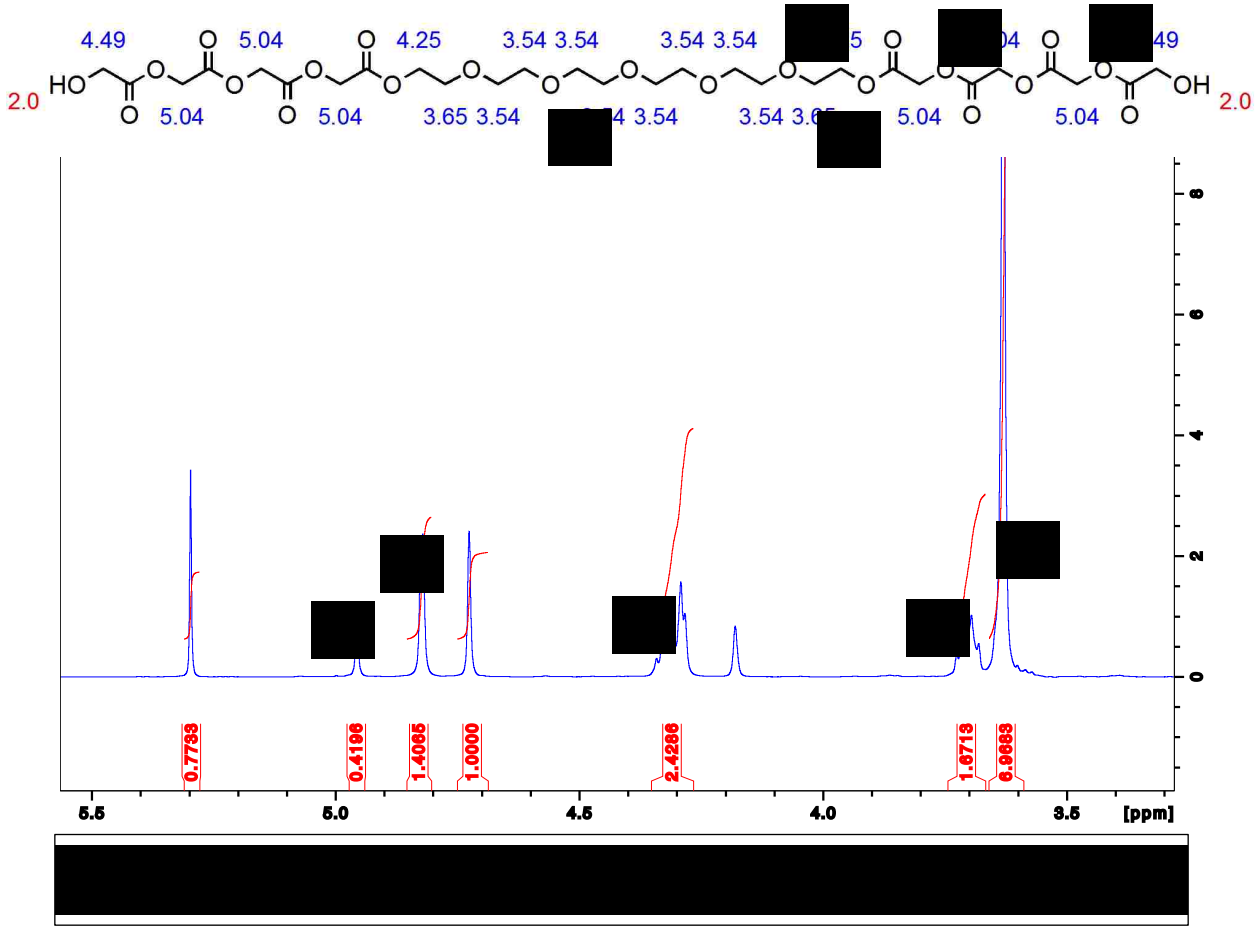

The analysis of the glycolide-PEG diol indicates poor conjugation of the glycolide to the PEG. Ring-opening polymerizations are also sensitive to water and that could have been a factor. Additionally, I used the same conditions for the glycolide reaction as I did for the caprolactone reaction. As glycolide is more reactive that caprolactone, the temperature and duration of the reaction may have been overkill. This would lead to formation of my intended product, but then thermal degradation of the glycolide units off the ends.

Next steps

The obvious next step is to synthesize the glycolide crosslinker correctly. Although water was the main culprit with this polymer, there is room for optimization on the ring opening polymerization of glycolide with PEG. The reaction was run with the same conditions as the caprolactone reaction, which may have been too hot and too long for the quicker reacting glycolide. Once it is properly synthesized, the degradation kinetics could be assessed. Additionally, it would be interesting to see if combining a quick degrading crosslinker with a slow degrading initiator would allow for more fine tuning of the overall degradation kinetics of the scaffold. For an *in vivo* implantation study, the scaffolds should be polymerized in the presence of gold nanoparticles which will aid in determining the original boundary of the implant. Another interesting study would be to make thicker scaffolds to determine if there is a maximum distance that cells are able to infiltrate.

Materials

Materials used in this study were used as received, unless otherwise noted. Dichloromethane (Fisher, D151-4, CAS# 75-09-2), anhydrous dichloromethane (Sigma-Aldrich, 270997-1L, CAS# 75-09-2), anhydrous tetrahydrofuran (Sigma-Aldrich, 401757, CAS# 109-99-9), anhydrous dimethyl sulfoxide (Sigma-Aldrich, 276855-2L, CAS# 67-68-5), methanol (Fisher,

A452-4, CAS# 67-56-1), and pentane (Fisher, P399-1, CAS# 109-66-0) were used as solvents. Chloroform-D (Aldrich, 151831-50G, CAS# 865-49-6) and dimethyl sulfoxide-d_6 (Aldrich, 151874-25G, CAS# 2206-27-1) were used as NMR solvents. Molecular sieves (Fisher, M514-500, CAS# 1344-00-9) were used to dry PEG. Sodium bicarbonate (Fisher, S233-500G, CAS# 144-55-8), sodium carbonate (Fisher, S263-500G, CAS# 497-19-8), sodium azide (Fisher, S227-100, CAS# 26628-22-8), and phosphate-buffered saline (Sigma, P5368-10PAK) were used to make buffers and anhydrous sodium sulfate (Fisher, S421-500, CAS# 7757-82-6) was used to dry polymer solutions. Whatman qualitative filter paper, grade 4 (Sigma-Aldrich, WHA1004-042) were used to filter products. Poly-ethylene glycol 300 (Aldrich, 202371-250G, 25322-68-3), glycolide (Sigma, G1796-25, CAS# 502-97-6), and ε-caprolactone (Aldrich, 704067, CAS# 502-44-3) were raw materials for the degradable core. Poly-ethylene glycol was dried using molecular sieves and heating to 120°C under vacuum. Tin (II) ethylhexanoate (Sigma, S3252-100G, CAS# 301-10-0), methacryloyl chloride (Sigma-Aldrich, 64120-50ML, CAS# 920-46-7), α-bromoisobutyryl bromide (Aldrich, 252271-100G, CAS# 20769-85-1), and triethylamine (Sigma-Aldrich, T0886-100ML, CAS# 121-44-8) were used to prepare the degradable ATRP initiator and degradable crosslinker. Ascorbic acid (Fluka, 95209, CAS# 50-81-7), 2,2′-bipyridyl (Aldrich, D216305-100G, CAS# 366-18-7), copper (I) chloride (Sigma-Aldrich, 224332-25G, CAS# 7758-89-6), and 2-hydroxyethyl methacrylate (Polysciences Inc., 04675-500, CAS# 868-77-9) were used in the ARGET ATRP reaction. Poly-methyl methacrylate beads (TA40, ART# 6399, Batch PS 1640) used in this study were 40μm in diameter.

Methods

Bead cake construction

To construct the mold for the controlled pore-size scaffolds, two microscope slides are assembled with a 1mm Teflon spacer between them. Into this space, monodisperse 40μm linear poly-methyl methacrylate beads are added. This mold is placed into a sonicator for one hour to pack the beads into a close-packed hexagonal arrangement. After sonication, the mold goes into an oven at 175°C for 20 hours to sinter the beads together and form the interconnections between pores. These interconnects are ~30% the size of the beads (14μm).

Non-degradable pHEMA scaffold construction

To form a non-degradable, porous poly-HEMA scaffold, first the monomer mix is created. It is composed of the monomer, a crosslinker, a UV initiator, and solvent. 1mL of 2-hydroxyethyl methacrylate is combined with 50μL of tetraethyleneglycol dimethacrylate and 5mg of Irgacure 651. After the initiator dissolves, 1mL of water is added and mixed. This solution is used to infiltrate the pre-formed bead cakes. The solution is pipetted through the opening at the top of the slide mold. After filling, the scaffolds are placed under vacuum to remove any air pockets between the beads. The monomer mix is then polymerized under UV light for six minutes, flipped, and polymerized for an additional six minutes. The porous scaffold is now formed and the poly-methyl methacrylate beads need to be dissolved. This occurs in a soxhlet with dichloromethane in constant reflux over the course of four days. After the soxhlet treatment, the scaffolds are soaked in acetone for two days. The scaffolds are transitioned into 70% ethanol for two days and then into water for two days. Once they have soaked in water, the scaffolds are complete. They can be punched into disks or lyophilized for scanning electron microscope analysis.

Caprolactone-based polymers

Synthesis conditions

To synthesize the core, 6g (0.02 moles) dried PEG-300 was weighed into a round-bottomed flask with 22.828g (0.20 moles) ε-caprolactone. This was purged with nitrogen and set to stir in an oil bath. After mixing, 0.05 wt% (14.4mg, 11.5μL) stannous (II) ethylhexanoate is added to catalyze the reaction. The reaction is placed under vacuum and heated to 200°C for two hours. The reaction is then cooled to 160°C and allowed to react for an additional four hours. The reaction is then cooled to room temperature. To purify the reaction, the core is dissolved in ~30mL anhydrous dichloromethane. This solution is then extracted with equal volumes of pentane three times to remove unreacted caprolactone and catalyst. Residual solvent is evaporated under vacuum at room temperature. This is stored under nitrogen at -20°C. The target product from this reaction should have a molecular weight of 1440g/mole.

ATRP initiator synthesis

To form the poly-caprolactone ATRP initiator from the core, 13.53g (9.4mmoles) of the core is weighed into a round-bottomed flask and dissolved in 60mL of anhydrous tetrahydrofuran under nitrogen flow. 6.55mL (46.9mmoles) triethylamine is stirred in. 2.9mL (23.4mmoles) α-bromoisobutyryl bromide is added under nitrogen. This is allowed to react at room temperature overnight. The reaction is then poured over a Buchner filter with Whatman paper #4 to remove the precipitated triethylamine salt. The tetrahydrofuran is evaporated under vacuum and the product is dissolved in 70mL dichloromethane. This is extracted three times with a saturated sodium bicarbonate solution and three times with water. The product is dried over sodium sulfate and the dichloromethane is evaporated under vacuum at room temperature. The ATRP initiator is stored under nitrogen at -20°C.

Crosslinker synthesis

To form the poly-caprolactone crosslinker from the core, 13.53g (9.4mmoles) of the core is weighed into a round-bottomed flask and dissolved in 75mL anhydrous dichloromethane under nitrogen flow. 6.55mL (46.9mmoles) triethylamine is stirred in and the mix is cooled to 0°C in an ice bath. 2.28mL (23.4mmoles) methacryloyl chloride is mixed with 10mL anhydrous dichloromethane in an additional funnel above the round-bottomed flask with the degradable core and triethylamine. This is added dropwise to the reaction over one hour. The reaction is allowed to react for 12 hours at 0°C and an additional 12 hours at room temperature. The reaction is then poured over a Buchner filter with Whatman paper #4 to remove the precipitated triethylamine salt. The product is extracted three times with a saturated sodium bicarbonate solution and three times with water. The product is dried over sodium sulfate and the dichloromethane is evaporated under vacuum at room temperature. The crosslinker is stored under nitrogen at -20°C.

ATRP reaction

To prepare the ATRP reaction mix, 1mL (8.22mmoles) of 2-hydroxyethyl methacrylate was added to 173.7mg (0.107mmoles) of the synthesized degradable poly-caprolactone ATRP initiator and 388.7mg (0.246mmoles, 3%mol of HEMA) of the synthesized degradable poly-caprolactone crosslinker. 1mL of anhydrous dimethyl sulfoxide is added as a solvent. 83.4mg (0.535mmoles) of 2,2′-bipyridyl is dissolved into the mix by vortex. This mix is bubbled with argon for one hour to remove oxygen. 21.2mg (0.214mmoles) of copper (I) chloride is added to start the reaction. This mix is used to infiltrate the previously prepared bead cakes to cast into a porous scaffold or cast into a solid slab. The reaction proceeds under nitrogen overnight at room temperature.

ARGET ATRP reaction

For the ARGET ATRP reaction mix, everything is the same except 20mg (0.113mmoles) ascorbic acid is added prior to the bubbling step.

Soxhlet

After the ATRP reaction, the scaffolds are placed into a soxhlet with dichloromethane under constant reflux for four days to dissolve the poly-methyl methacrylate beads. The scaffolds are then washed in acetone for two days, 70% ethanol for two days, and water for two days.

SEM of scaffolds

Scaffolds were punched into 6mm disks and freeze dried using a lyophilizer. Some disks were analyzed by scanning electron microscope after sputtering with Au/Pd.

Degradation

For the accelerated degradation study, solid disks made from Anna Galperin and Sarah Atzet's previously developed caprolactone based polymers were compared to solid and porous disks made from my synthesized caprolactone based polymers. The disks were lyophilized to get the initial dry mass. The disks were placed into 10mL bicarbonate buffer (100mM, pH 10.3) at 37°C in a shaker incubator (80rpm). Three samples were taken daily for one week for each condition. After degradation, samples were washed in water for 30 minutes and then lyophilized to get the final mass.

I also assessed the degradation of my caprolactone based polymers in PBS (150mM, pH 7.4) with 0.05%wt sodium azide over four months.

Glycolide-based polymers

Synthesis conditions

To synthesize the core, 6g (0.02 moles) dried PEG-300 was weighed into a round-bottomed flask with 11.6g (0.10 moles) glycolide under nitrogen. The mixture was heated in an oil bath to 90°C to melt the glycolide and combine. After the glycolide melted, 7μL (0.05%wt) stannous (II) ethylhexanoate was added and the reaction was put under vacuum. The reaction proceeded at 200°C for two hours and 160°C for an additional four hours. The reaction is then cooled to room temperature. To purify the reaction, the core is dissolved in ~30mL anhydrous dichloromethane. This solution is then extracted with equal volumes of pentane three times to remove any unreacted glycolide and catalyst. After purification, residual solvent is evaporated under vacuum at room temperature. This is stored under nitrogen at -20°C. The target product from this reaction should have a molecular weight of 880g/mole.

ATRP initiator synthesis

To form the poly-glycolic acid ATRP initiator from the core, 7g (7.95mmoles) of the core is weighed into a round-bottomed flask and dissolved in 75mL anhydrous tetrahydrofuran under nitrogen flow. 5.53mL (39.7mmoles) triethylamine is stirred in. 2.44mL (19.8mmoles) α-bromoisobutyryl bromide is added under nitrogen. This is allowed to react at room temperature overnight. The reaction is then poured over a Buchner filter with Whatman paper #4 to remove the precipitated tritethylamine salt. The tetrahydrofuran is evaporated under vacuum and the product is dissolved in 70mL dichloromethane. This is extracted three times with a saturated sodium bicarbonate solution and three times with water. The product is dried over sodium sulfate and the dichloromethane is evaporated under vacuum at room temperature. The ATRP initiator is stored under nitrogen at -20°C.

Crosslinker synthesis

To form the poly-glycolic acid crosslinker form the core, 7g (7.95mmoles) of the core is weighed into a round-bottomed flask and dissolved in anhydrous dichloromethane under nitrogen flow. 5.53mL (39.7mmoles) triethylamine is stirred in and the mix is cooled to 0°C in an ice bath. 1.93mL (19.8mmoles) methacryloyl chloride is mixed with 10mL anhydrous dichloromethane in an additional funnel above the round-bottomed flask. This is added dropwise to the reaction over one hour. The reaction is allowed to react for 12 hours at 0°C and an additional 12 hours at room temperature. The reaction is then poured over a Buchner filter with Whatman paper #4 to remove the precipitated triethylamine salt. The product is extracted three times with a saturated sodium bicarbonate solution and three times with water. The product is dried over sodium sulfate and the dichloromethane is evaporated under vacuum at room temperature. The crosslinker is stored under nitrogen at -20°C.

ARGET ATRP reaction

To prepare the ARGET ATRP reaction mix, 1mL (8.22mmoles) of 2-hydroxylethyl methacrylate was added to 126mg (0.107mmoles) of the synthesized degradable poly-glycolic acid ATRP initiator and 250mg (0.246mmoles) of the synthesized degradable poly-glycolic acid crosslinker. 1mL of anhydrous dimethyl sulfoxide is added as a solvent. 83.4mg (0.535mmoles) of 2,2′-bipyridyl and 20mg (0.113mmoles) ascorbic acid is dissolved into the mix by vortex. This mix is bubbled with argon for one hour to remove oxygen. 21.2mg (0.214mmoles) of copper(I) chloride is added to start the reaction. This mix is used to cast solid or porous polymer slabs. The reaction proceeds under nitrogen overnight at room temperature.

Bibliography

1. Anderson, J.M., Rodriguez, A., and Chang, D.T. (2008). Foreign body reaction to biomaterials. Seminars in Immunology *20*, 86–100.
2. Atzet, S., Curtin, S., Trinh, P., Bryant, S., and Ratner, B. (2008). Degradable Poly(2-hydroxyethyl methacrylate)- *co* -polycaprolactone Hydrogels for Tissue Engineering Scaffolds. Biomacromolecules *9*, 3370–3377.
3. Berthiaume, F., Maguire, T.J., and Yarmush, M.L. (2011). Tissue Engineering and Regenerative Medicine: History, Progress, and Challenges. Annual Review of Chemical and Biomolecular Engineering *2*, 403–430.
4. Brown, B.N., Ratner, B.D., Goodman, S.B., Amar, S., and Badylak, S.F. (2012). Macrophage polarization: An opportunity for improved outcomes in biomaterials and regenerative medicine. Biomaterials *33*, 3792–3802.
5. Fukano, Y., Usui, M.L., Underwood, R.A., Isenhath, S., Marshall, A.J., Hauch, K.D., Ratner, B.D., Olerud, J.E., and Fleckman, P. (2010). Epidermal and dermal integration into sphere-templated porous poly(2-hydroxyethyl methacrylate) implants in mice. Journal of Biomedical Materials Research Part A *9999A*, NA-NA.
6. Lee, J.M., and Kim, Y.J. (2015). Foreign Body Granulomas after the Use of Dermal Fillers: Pathophysiology, Clinical Appearance, Histologic Features, and Treatment. Archives of Plastic Surgery *42*, 232.
7. Long, T.J., Takeno, M., Sprenger, C.C., Plymate, S.R., and Ratner, B.D. (2013). Capillary Force Seeding of Sphere-Templated Hydrogels for Tissue-Engineered Prostate Cancer Xenografts. Tissue Engineering Part C: Methods *19*, 738–744.
8. Madden, L.R., Mortisen, D.J., Sussman, E.M., Dupras, S.K., Fugate, J.A., Cuy, J.L., Hauch, K.D., Laflamme, M.A., Murry, C.E., and Ratner, B.D. (2010). Proangiogenic scaffolds as functional templates for cardiac tissue engineering. Proceedings of the National Academy of Sciences *107*, 15211–15216.
9. Marshall, A.J., Irvin, C.A., Barker, T., Sage, E.H., Hauch, K.D., and Ratner, B.D. Biomaterials with tightly controlled pore size that promote vascular in-growth. 2.
10. Meyer, U. (2009). The History of Tissue Engineering and Regenerative Medicine in Perspective. In Fundamentals of Tissue Engineering and Regenerative Medicine, (Springer, Berlin, Heidelberg), pp. 5–12.
11. O'Brien, F.J. (2011). Biomaterials & scaffolds for tissue engineering. Materials Today *14*, 88–95.
12. Portou, M.J., Baker, D., Abraham, D., and Tsui, J. (2015). The innate immune system, toll-like receptors and dermal wound healing: A review. Vascular Pharmacology *71*, 31–36.
13. Qazi, T.H., Mooney, D.J., Pumberger, M., Geißler, S., and Duda, G.N. (2015). Biomaterials based strategies for skeletal muscle tissue engineering: Existing technologies and future trends. Biomaterials *53*, 502–521.
14. Ratner, B.D. (2002). Reducing capsular thickness and enhancing angiogenesis around implant drug release systems. Journal of Controlled Release *78*, 211–218.
15. Ratner, B.D. (2016). A pore way to heal and regenerate: 21st century thinking on biocompatibility. Regenerative Biomaterials *3*, 107–110.
16. Saini, M. (2015). Implant biomaterials: A comprehensive review. World Journal of Clinical Cases *3*, 52.

17. Sawhney, A.S., Pathak, C.P., and Hubbell, J.A. (1993). Bioerodible hydrogels based on photopolymerized poly(ethylene glycol)-co-poly(.alpha.-hydroxy acid) diacrylate macromers. Macromolecules *26*, 581–587.
18. Sridharan, R., Cameron, A.R., Kelly, D.J., Kearney, C.J., and O'Brien, F.J. (2015). Biomaterial based modulation of macrophage polarization: a review and suggested design principles. Materials Today *18*, 313–325.
19. Sussman, E.M., Halpin, M.C., Muster, J., Moon, R.T., and Ratner, B.D. (2014). Porous Implants Modulate Healing and Induce Shifts in Local Macrophage Polarization in the Foreign Body Reaction. Annals of Biomedical Engineering *42*, 1508–1516.
20. Underwood, R.A., Usui, M.L., Zhao, G., Hauch, K.D., Takeno, M.M., Ratner, B.D., Marshall, A.J., Shi, X., Olerud, J.E., and Fleckman, P. (2011). Quantifying the effect of pore size and surface treatment on epidermal incorporation into percutaneously implanted sphere-templated porous biomaterials in mice. Journal of Biomedical Materials Research Part A *98A*, 499–508.
21. Wynn, T.A., and Vannella, K.M. (2016). Macrophages in Tissue Repair, Regeneration, and Fibrosis. Immunity *44*, 450–462.
22. Young, C.-D., Wu, J.-R., and Tsou, T.-L. (1998). Fabrication and characteristics of polyHEMA artificial skin with improved tensile properties. Journal of Membrane Science 11.
23. Zaulyanov, L., and Kirsner, R.S. (2007). A review of a bi-layered living cell treatment (Apligraf) in the treatment of venous leg ulcers and diabetic foot ulcers. Clinical Interventions in Aging *2*, 93–98.